Contact Engineering for Dual-Gate MoS_2 Transistors with O_2 Plasma Exposure

P. Bolshakov[1], C. M. Smyth[1], A. Khosravi[1], P. Zhao[1], A. Azcatl[1], G. Mirabelli[2],
P. K. Hurley[2], C. L. Hinkle[1], R. M. Wallace[1], and C. D. Young[1]
1. University of Texas at Dallas, Richardson, TX, USA
2. Tyndall National Institute, University College Cork, Cork, Ireland

Abstract - *Transition metal dichalcogenides (TMDs) are a sub-group of 2D materials being investigated for their potential use in low-power, high-mobility circuits. Schottky electrical contacts thought to be formed by Fermi level pinning (FLP) at the contact metal/TMD interface continue to hinder progress towards Ohmic contacts for TMD devices. We investigate the role of photoresist residue on MoS_2 during and after fabrication of FETs using topographical, interfacial, and electrical characterization. When using an O_2 plasma exposure prior to contact metal deposition on MoS_2, we remove photoresist residue and form a quality TiO_x/MoS_2 contact. Dual-gate (DG) MoS_2 FETs with O_2 plasma exposure demonstrate a ~15× increase in mobility and a ~20× decrease in R_C.*

Device Fabrication and Characterization – Initially, atomic layer deposition (ALD) of Al_2O_3 (27 nm) at 250 ºC onto a p+ Si wafer was performed with subsequent deposition of Al for a backside contact as well as a 400 ºC forming gas anneal to reduce charge traps. This backside layer serves as the 'substrate' for few-layer MoS_2 flakes (4-8 nm) **[1]**. Using photolithography, source/drain contacts are defined and followed by e-beam evaporation of Ti/Au contacts with a lift-off process. For comparison, certain devices also had a direct O_2 plasma 5 sec exposure ("de-scum") at 50W to remove any photoresist residue prior to contact metal deposition. Electrical back-gate measurements were performed. Then, a 300 ºC UHV anneal and 15 minute in-situ UV-ozone surface treatment was performed, followed by ALD of a Al_2O_3/HfO_2 (3nm/6nm) gate oxide at 200 ºC **[2]**,**[3] and** Pd/Au top-gate deposition. AFM and XPS were used to investigate the topographical and interfacial changes occurring on the MoS_2 layer throughout the contact formation process. DG sweeping of both the back-gate and the top-gate during electrical characterization helped achieve optimal device performance **[4]**.

Results and Discussion – Without O_2 plasma exposure prior to Ti/Au deposition on MoS_2, the I_D-V_D of MoS_2 FETs demonstrates non-linearity (Fig.1c), whereas those with exposure consistently show linear behavior (Fig.1d). This suggests that better carrier injection is achieved at the contacts as a result of the O_2 plasma exposure. AFM was used to investigate the MoS_2 surface as-exfoliated, post-photoresist development, and post-O_2 plasma exposure where the topographical images (Fig.2) indicate large photoresist island formation up to 20 nm in height and 50 nm in diameter during the lift-off process. This suggests the resist residue will likely cause discontinuous contact between the Ti contact metal and the underlying MoS_2. After O_2 plasma exposure, the large clusters of photoresist are removed, resulting in a roughness comparable to that of as-exfoliated MoS_2. This demonstrates that the 5 sec O_2 plasma exposure post-development is enough to remove a majority of the residue prior to metal deposition. XPS analysis after exfoliation, development, plasma exposure, and Ti deposition in high-vacuum (HV) helps further elucidate the role of photoresist residue, O_2 plasma, and the subsequent chemistry formed after Ti deposition on MoS_2 (Fig.3a-b). The initial comparison between as-exfoliated MoS_2 and after resist deposition/removal indicates a Fermi level shift towards the conduction band (E_C) edge, suggesting FLP near the E_C is due to photoresist residue. Two different MoS_2 samples are used to demonstrate FLP at roughly the same energy near the E_C, regardless of the initial as-exfoliated MoS_2 Fermi level position (Fig.3c). After O_2 plasma exposure, the XPS spectra indicates a Fermi level shift to its as-exfoliated value and formation of MoO_x species. This suggests that a combination of hole injection by MoO_x and removal of the residue causes the Fermi level shift towards the valence band after O_2 plasma. Subsequent Ti deposition indicates that the contact metal scavenges the oxygen species, reducing the MoO_x to form TiO_x (Fig.3a-b), enhancing carrier injection likely due to a low conduction band offset of TiO_2 with MoS_2 **[5]**. The removal of the residue coupled with the Ti oxygen gettering effect enables the dual-role of the short O_2 plasma exposure prior to contact metal deposition and formation of higher performing n-type contacts on MoS_2. After metal deposition and lift-off, the back-gate MoS_2 FETs intuitively have photoresist residue on the MoS_2 channel surface. Electrical characterization before and after O_2 plasma exposure at the channel indicates reduction in the OFF current of I_D-V_G (Fig.4c), suggesting that the photoresist residue may constitute a net positive charge, in similar way to fixed positive oxide charge after high-k dielectric deposition on MoS_2 **[6],[7]**. Using O_2 plasma to remove the excess carriers generated results in a reduction of saturation current in the I_D-V_D (Fig.4d). After top-gate stack formation, DG MoS_2 FETs with and without O_2 plasma exposure at the contacts only demonstrate non-linear and linear I_D-V_D (Fig.5b), respectively, even after the thermal heating from the UHV anneal and the ALD. Furthermore, the I_D-V_G (Fig.5c) shows major improvements in mobility (Fig.5d) and R_C due to formation of higher quality contacts. Overall, the results show that device fabrication induced contaminants like photoresist can significantly hamper MoS_2 transistor performance if not properly eliminated.

Acknowledgment - This work was supported in part by the US/Ireland R&D Partnership (UNITE) under the NSF award ECCS-1407765, and the NSF CAREER award ECCS-1653343. This work was also supported in part by Semiconductor Research Corporation (SRC) as the NEWLIMITS center and NIST through award number 70NANB17H041.

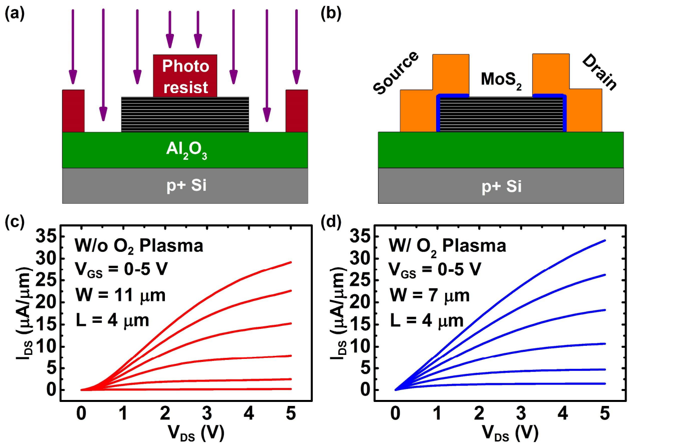

Figure 1. **(a)** Graphic illustrating the O_2 plasma exposure at the exposed contact areas after development of the photoresist and **(b)** the final back-gate MoS_2 FET structure. **(c)** The I_D-V_D of MoS_2 FET without and **(d)** with O_2 plasma exposure.

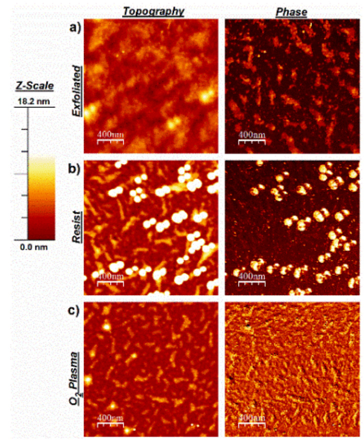

Figure 2. AFM topography and phase images obtained from a MoS_2 flake after **(a)** exfoliation, **(b)** photolithography processing, and **(c)** O_2 plasma exposure.

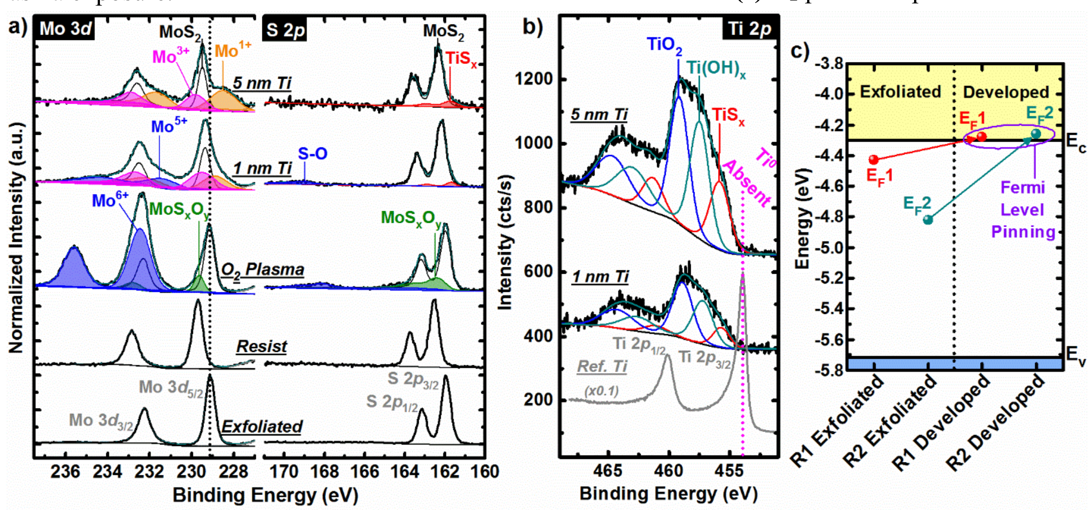

Figure 3. XPS core level spectra (**(a)** Mo 3*d*, S 2*p*, and **(b)** Ti 2*p*) obtained from bulk MoS_2 after exfoliation, photolithographic processing, 5 s O_2 plasma, 1 nm Ti deposition, and 5 nm Ti deposition. **(c)** Band alignment of two bulk MoS_2 crystals after exfoliation and photolithographic processing according to the measured valence band offset.

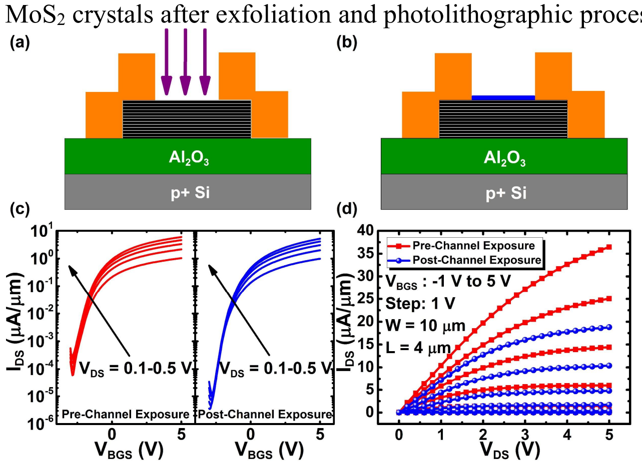

Figure 4. **(a)** Graphic illustrating O_2 plasma exposure at the exposed channel area and **(b)** the back-gate MoS_2 FET after channel exposure. **(c)** Comparison of I_D-V_G and **(d)** I_D-V_D of the same BG MoS_2 FET before and after exposure.

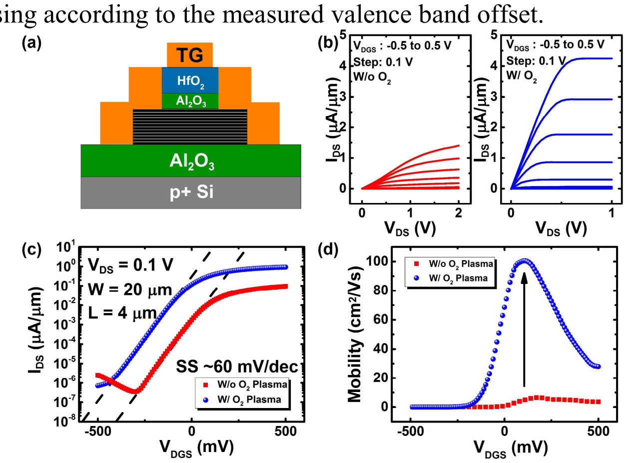

Figure 5. **(a)** Graphic cross-section of a DG MoS_2 FET. **(b)** Comparison of I_D-V_D and **(c)** I_D-V_G of DG MoS_2 FETs without and with O_2 plasma exposure at the contacts only. **(d)** Extracted mobility demonstrating a ~15× improvement.

[1]P. Bolshakov *et al.*, *Appl. Phys. Lett.*, vol. 111, no. 3, p. 032110, Jul. 2017. **[2]**A. Azcatl *et al.*, *Appl. Phys. Lett.*, vol. 104, no. 11, p. 111601, 2014.**[3]**A. Azcatl *et al.*, *2D Mater.*, vol. 2, no. 1, p. 014004, Jan. 2015.**[4]**P. Bolshakov *et al.*, *Appl. Phys. Lett.*, vol. 253502, no. 25, p. 253502, Jun. 2018.**[5]**N. Kaushik *et al., ACS Appl. Mater. Interfaces*, vol. 8, no. 1, pp. 256–263, Jan. 2016.**[6]**J. Na *et al.*, *Nanoscale*, vol. 6, no. 1, pp. 433–41, 2014.**[7]**T. Li *et al., AIP Adv.*, vol. 5, no. 5, p. 057102, 2015.